

Coronal Structure: Legacy of EUVE

NASA Grant NAG5-7224

Final Report

For the period 15 April 1998 to 14 April 2000

Principal Investigator

Dr. Andrea K. Dupree

November 2000

Prepared for

National Aeronautics and Space Administration

Washington, D.C. 20546

Smithsonian Institution

Astrophysical Observatory

Cambridge, Massachusetts 02138

<p>The Smithsonian Astrophysical Observatory is a member of the Harvard-Smithsonian Center for Astrophysics</p>

The NASA Technical Officer for this Grant is Dr. Donald K. West, Code 684.1, Laboratory for Astronomy and Solar Physics, Space Sciences Directorate, NASA/Goddard Space Flight Center, Greenbelt, MD 20771.

Coronal Structure: Legacy of EUVE

Spectra of cool stars have been acquired with EUVE both through the Guest Observer Program and from the EUVE data archive, in order to compile a complete set of observations of this major class of objects.

Analysis of the extreme ultraviolet spectra of cool stars has revealed a surprising new view of stellar coronas that we are just now beginning to understand. The structures are of high density, high temperature, small, and stable, and demand high magnetic fields and continuous energy input for their existence. This is a totally unexpected condition in the extremes of a hot corona. These features cannot yet be matched by theory. While loop models are reasonably satisfactory in matching the solar case, they fail in reproducing the stellar emission measure distributions. Something is radically different in these stellar coronas (perhaps due to rotation?), and simple extrapolation from the Sun does not work.

Electron densities at coronal temperatures have been inferred from appropriate line ratios. These include iron ions ranging from Fe XIII to Fe XXII. *An early striking discovery from EUVE spectra is the presence of very high densities ($\sim 10^{12} \text{cm}^{-3}$) at high temperatures ($\sim 6 \times 10^6 \text{K}$).* Moreover, spectra from an active RSCVn-type binary, λ And reveal density enhancements of about a factor of 6 above these already high values during a stellar flare. Electron densities for a number of stars demonstrate that the transition regions and coronas are not at constant pressure. Because several regimes of pressure may coexist, in what apparently are equilibrium conditions, magnetic fields are necessary to confine the plasma. Simple energetics of an ion in a hot plasma also show that a star with low gravity can not retain a hot corona. And direct measurement of the wavelength of the Fe XXI ($\lambda 1354$) line in 2 sources (HR 1099 and Capella) with HST/GHRS demonstrates that the hot plasma is associated with photospheric velocity of a star, and not expanding.

The stellar electron densities at high temperatures ($T \sim 10^7 \text{K}$) are high, $10^{12} - 10^{13} \text{cm}^{-3}$, when compared to coronal structures found on the Sun. The scale of the coronal structures can be estimated when N_e is known. The electron density at a given temperature, which in combination with the emission measure, $EMD \approx N_e^2 \Delta V_T$, assesses the linear scale, viz. $(\Delta V_T)^{1/3}$. In well-studied cases such as Capella, 44 Boo, and λ And, the scales are much less than a stellar radius. These coronal features must have continued heating since the radiative cooling times ($\tau_{rad} = 3n_e kT / n_e^2 \Psi(T)$, and $\Psi(T) \approx 5 \times 10^{-23} \text{erg s}^{-1} \text{cm}^{-3}$) are short – on the order of minutes for these high densities.

A graduate student, J. Sanz-Forcada, participating in the Smithsonian Predoctoral program is basing a major part of his Ph.D. thesis on EUVE spectra in order to provide a similar comprehensive analysis of the cool star targets of EUVE. A brief version of a longer paper submitted to the ApJ, is attached.

Publications and Presentations Associated with EUVE
Funded in part under NAG5-7224: 04/15/98–4/14/00

Extreme Ultraviolet Explorer Observations of the W Ursae Majoris Contact Binary 44i Boo: Coronal Structure and Variability, N. S. Brickhouse & A. K. Dupree, 1998, ApJ, **502**, 918.

EUVE Observations of 44i Boo: Evidence for Localized Emission, N. S. Brickhouse & A. K. Dupree, 1998, in 10th Cambridge Workshop on Cool Stars, Stellar Systems, and the Sun, ASP Conf. Series, **154**, R. Donahue & J. Bookbinder (eds), 993

Cool Stars: Imaging and Spectroscopy, A. K. Dupree, 1999, in ASP Conf. Ser. **164**, Ultraviolet-Optical Space Astronomy Beyond HST,

Coronal Structure and Abundances of *Capella* from Simultaneous *EUVE* and *ASCA* Spectroscopy, N. S. Brickhouse, A. K. Dupree, R. J. Edgar, D. A. Liedahl, S. A. Drake, N. E. White, & K. P. Singh, 2000, ApJ, **530**, 387

Coronal Physics of Cool Stars, A. K. Dupree 2000, Invited Review in Cool Stars 11: ASP Conf. Series, in press.

EUVE Observations of Lambda Andromedae, J. Sanz-Forcada, N. S. Brickhouse, & A. K. Dupree 2000, in Cool Stars 11: ASP Conf. Series, in press.

Capella: Coronal Variability from EUVE, A. K. Dupree, N. S. Brickhouse, & J. Sanz-Forcada, 1999, BAAS, Mtg. 195, 76.03

AAS HEAD Meeting: The 1998 ASCA/EUVE Campaign on the Active Binary UX Ari; S. A. Drake, N. E. White, A. K. Dupree, N. S. Brickhouse, J. Sanz-Forcada, & K. P. Singh, 1999, BAAS, **31**, 706.

AAS HEAD Meeting: The ASCA/EUVE Campaign: Structure and Abundances of the Eclipsing Binary AR Lac, N. S. Brickhouse, A. K. Dupree, J. Sanz-Forcada, S. A. Drake, N. E. White, & K. P. Singh, 1999, BAAS, **31**, 706

EUVE Observations of Lambda Andromedae

J. Sanz-Forcada^{1,2}, N.S. Brickhouse¹, and A.K. Dupree¹

Abstract.

Extreme ultraviolet spectra ($\lambda\lambda$ 70–740) and light curves ($\lambda\lambda$ 75–175) of the spectroscopic binary system λ And (HD 222107), were obtained with the *Extreme Ultraviolet Explorer* satellite (*EUVE*) in July and August 1997. Two flares were detected during the observations which spanned 15 days, or almost three-quarters of the orbital period of 20.5 days. The Emission Measure Distribution (EMD) of λ And derived from a line-based analysis, shows an increasing slope with the temperature from 3.1×10^6 K through 2.0×10^7 K, as well as a remarkable “bump” around $T_e \sim 10^{6.9}$ K. During the flares small changes were detected in both the general slope of the EMD and the height of the bump, but the bump remained very stable in its temperature. Electron densities of $N_e \sim 10^{12.7} \text{ cm}^{-3}$ are indicated at temperatures of 10^7 K using Fe XXI and Fe XXII emission features.

1. Introduction

λ And (HR 8961, HD 222107) is a nearby non-eclipsing spectroscopic RS CVn system ($d = 25.81 \text{ pc}$; Perryman et al. 1997) in whose spectrum only a G8IV–III star is seen. RS CVn systems are characterized by the strong emission in ultraviolet, EUV, and X-ray wavelengths because their high rotation rates cause a vigorous magnetic dynamo. These are interesting targets for the research in coronal structure, and so are frequent targets for space observatories (see Mitrou et al. 1997, Dempsey et al. 1993). λ And is the second brightest system of the RS CVn group, and unusually, has a very different photometric period (54.33 d; Perryman et al. 1997) from the orbital period (20.5212 d; Walker 1944). It is expected that the most of the activity seen comes from the primary star in the system, as the secondary is not detected spectroscopically. This star also shows a low rotation rate ($v \sin i = 6.5 \text{ km s}^{-1}$; Donati et al. 1995), and it is likely (Henry et al. 1995) to have differential rotation based on the variability found in the photometric period. Henry et al. (1995) calculate an activity period of 11.1 years, and Baliunas & Dupree (1982) find an anti-correlation between Ca II line intensity and visual magnitude variations, exhibiting maximum strength in the Ca II lines in coincidence with the faintest phases of the photometric phase. This suggests a relation between the chromospheric emissions and the

¹Harvard-Smithsonian Center for Astrophysics (USA)

²Departamento de Astrofísica. Universidad Complutense de Madrid (Spain)

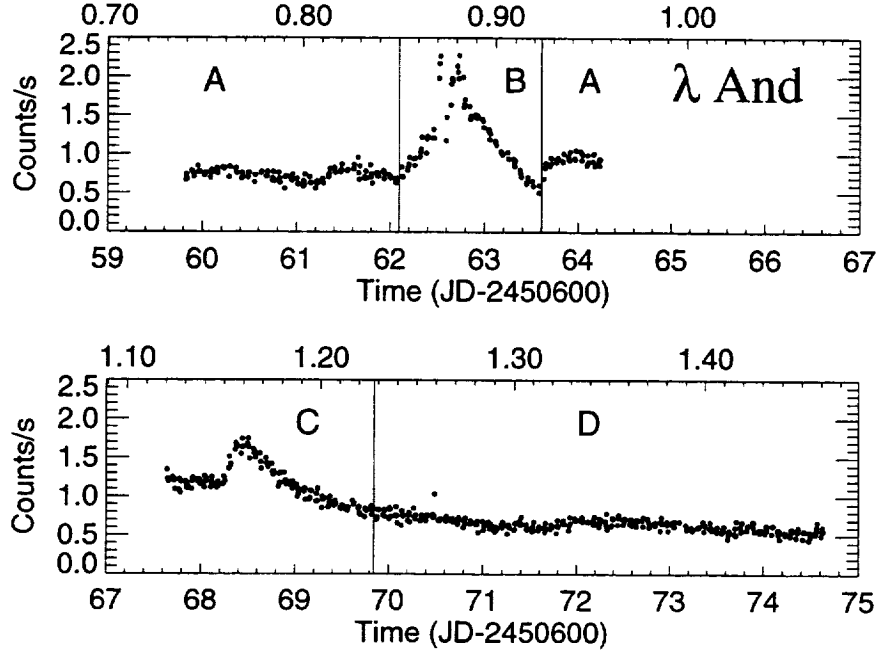


Figure 1. DS EUVE Light Curve (600 s. binning) for λ And as a function of Julian Date (lower axis) and orbital phase (upper axis) for July/August 1997. At orbital phase 1.0 the unknown secondary star is located behind the primary star. Points with S/N less than 5 were rejected.

presence of spots in the photosphere of λ And (more dark spots in coincidence with stronger Ca II line emission).

Ortolani et al. (1997) analyze ASCA and ROSAT λ And data. For ASCA they find that the spectra are well described using a 2-T model, but applying a 2-T model to the ROSAT data gives lower temperatures. Osten & Brown (1999) study the general properties of the EUVE flares in several RS CVn systems among which λ And is included.

The *EUVE* (*Extreme Ultraviolet Explorer*) satellite is able to detect lines ($\lambda\lambda$ 70–700) formed in material at high temperatures, ranging from 10^6 to 2×10^7 K, thus allowing coronal structure to be determined. Observing time on EUVE was made available through the Guest Observer Program.

2. Observations

The EUVE observations were taken in two runs from July 30 – August 3, and August 7 – August 14 1997. Total time on the target amounted to 280 ks. The time spanned by these observations was 15 days. EUVE spectrographs cover the spectral range 70–175 Å, 150–350 Å and 300–700 Å for the short-wavelength (SW), medium-wavelength (MW) and long-wavelength (LW) spectrometers respectively. The Deep Survey Imager (DS) has a bandpass of 80–180 Å.

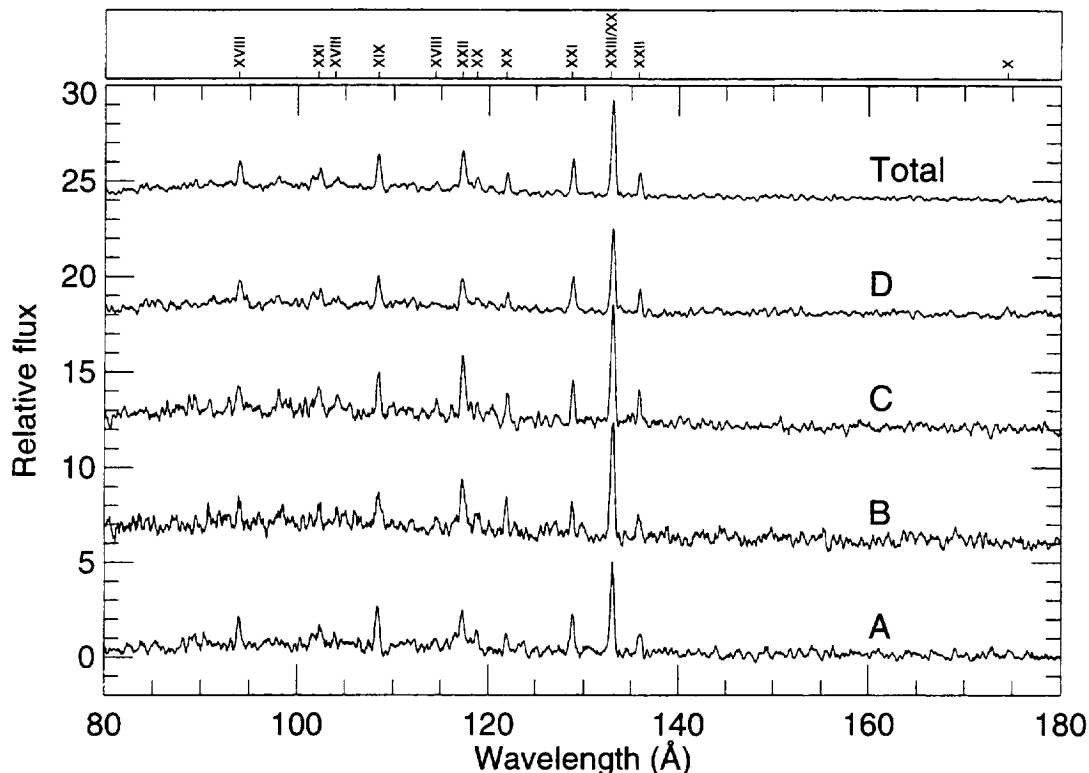


Figure 2. EUVE SW spectrum for λ And for the four time intervals (ABCD) and the summed spectrum. Ion stages of iron are marked in the top panel.

The EUVE light curve was built from the DS image, by taking a circle of radius 22 pixels centered on the source, and subtracting the sky background within an annulus of radii at the pixel 25 and 100 from the center. It was performed with IRAF standard procedures, the package EUV 1.8, and a binning of 600 s. The variations observed in the light curve show λ And four different temporal states (denoted by A, B, C, D, with 66562, 32849, 60055, and 123464 s of exposure time respectively) (see Fig. 1). Spectra binned over the DS intervals were extracted from the three spectrographs. A summed spectrum was constructed from spectra A–D, which totaled 283,455 seconds.

3. Data analysis

The DS light curve from EUVE has been compared with the orbital and photometric periods. It doesn't show any cyclic variability, due in part to the existence of two strong changes in the star's flux. We interpret the strong changes as flares. The second flare has the typical exponential decay. But the first flare is a more atypical flare, with higher flux and a fast decay, in a quasi-symmetric way. V711 Tau showed also a similar behavior in September 1996 (Osten & Brown 1999).

Since the second observing segment begins with a higher flux at the beginning than the flux observed at the end of the first interval, it may indicate that

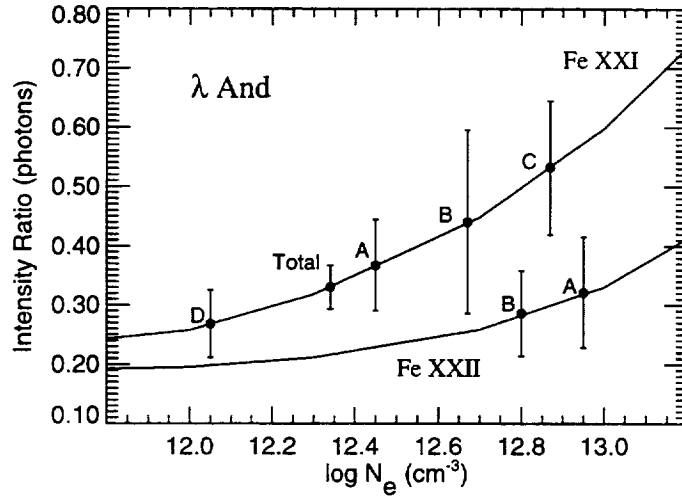


Figure 3. N_e derived from line ratio diagnostics from two different ionization stages of Fe. The line ratios shown are Fe XXI $\lambda 102.22/\lambda 128.73$ and Fe XXII $\lambda 114.41/\lambda 117.17$ for each spectral segment (A–D) and the total. The observed line ratios are plotted on the theoretical curves with 1- σ error bars representing the combined observational errors.

another flare occurred in the gap between the two intervals. The EUVE satellite was taken from our source to observe a target of opportunity and so we do not have direct observations of any event.

The EUVE spectra (Fig. 2) show a strong bremsstrahlung continuum below 130 Å. Lines between Fe XVIII and Fe XXIV ionization states occur in every spectrum, and also Fe XVI lines are found with poor S/N in segment D. To obtain fluxes of the emission lines we performed optimized extractions from the summed two-dimensional images by removing an averaged background evaluated on either side of the spectrum, using the software provided in IRAF and the EGODATA 1.18 reference data set.

To correct the theoretical fluxes for the interstellar hydrogen and helium continuum absorption, we used $\log N_H = 18.45 \pm 0.15 \text{ cm}^{-2}$ obtained from direct measure of hydrogen absorption in the Lyman α line profile with HST/GHRS (Wood et al. 1996), and a ratio He I/H I = 0.09 (Kimble et al. 1993).

The electron density in the corona of λ And has been inferred from the ratios Fe XXI $\lambda\lambda 102.22/128.73$ and Fe XXII $\lambda\lambda 114.41/117.17$, giving an average of the values in every segment and ion of $\log N_e (\text{cm}^{-3}) = 12.7$ (see Fig. 3). The iron line emissivities were corrected using this value for N_e . Atomic models for Fe XXI and Fe XXII were taken from Brickhouse et al. (1995).

We performed a Lined Based Analysis of the observed lines in order to calculate the EMD (emission measure distribution, $\int N_e N_H dV$, where N_e and N_H are electron and hydrogen densities, in cm^{-3}) that contributes to create the observed fluxes. We used the line emissivities calculated from Raymond (1988) for the IUE lines, and Brickhouse et al. (1995) for the EUVE iron lines. Theoretical fluxes were calculated (see Dupree et al. 1993, Brickhouse & Dupree

1998 and references therein), and then compared with the observed fluxes, in order to obtain the best EMD that fits the observed fluxes within a factor of two.

The EMD is shown in Fig. 4 for the spectra where the low temperature segment ($\log T(K) \lesssim 5.3$) is defined by the quiescent IUE spectrum for the segments A, D and the summed spectrum, and the flare IUE spectrum (Baliunas et al. 1984) is used for segments B and C. Data provided by Ortolani et al. (1997) have been included also in Fig. 4 to compare with ASCA and ROSAT results. Fig. 5 shows the comparison among the different segments.

4. Discussion

4.1. Light curve

The EUV light curve was obtained in the same epoch with photometric observations made by Wasatonic, R. & Guinan, E.F. (1999, private communication). According to their light curves, the TiO index³ is at a high level. The IR magnitude (at $\lambda\lambda 10240$) also shows a maximum brightness on the same dates, and the visual light curve shows a decreasing brightness as the TiO index grows slightly.

This suggests that the primary star of the system exhibits an increasing number of spots in coincidence with the first flare. After this first flare, the level of spottedness remains at high levels for the rest of our observations. The general behavior of the DS light curve shows a high level of activity until the decay of the second flare, in agreement with the values of N_e obtained from the ratios between iron lines (see below).

There is no EUV modulation associated with the orbital period. Flares occurred at orbital phases 0.87 and 0.16. No accurate rotational phase can be given as the rotation period changes slightly in this star from one epoch to another. From the data obtained by Wasatonic & Guinan, a rotational period of 54.11 days can be inferred from the visual light curve, close to the value given by Perryman et al. (1997).

4.2. Electron Density

The high level of bremsstrahlung continuum observable in all the segments for the SW spectrum is in agreement with the N_e values previously mentioned and with the presence of high ionization state lines, such as Fe XXIV. When we observe the evolution of the electron density using Fe XXI in the four segments (see Fig. 3), higher values of the density occur for the flare segment (C) in contrast with lower values for quiescent segments (D) and the summed spectrum. This behavior is consistent with the presence of the flares in segments B and C. Because λ And is in a quiescent state for most of the observation, the low density indicated by the summed spectrum is not surprising. Fe XXII ratios suggest a higher density than in the Fe XXI plasma, but we can not claim any change during the flare because of poor statistics.

³This index is useful to measure the likely presence of spots on the photosphere, a numerical increase in the TiO index corresponds to an increase in the TiO absorption bands at 7190 Å

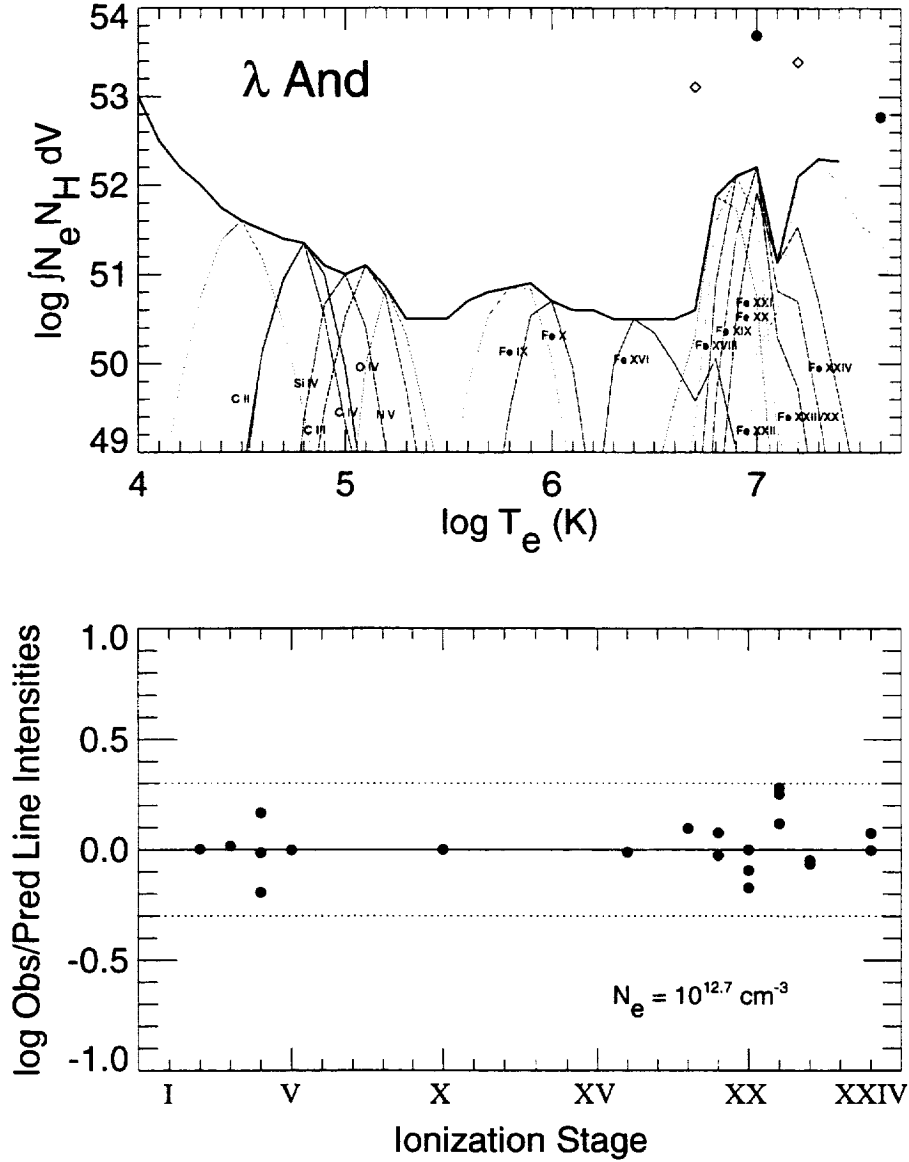


Figure 4. Upper figure: EMD for the total EUVE spectrum combined with the IUE quiescent spectrum. Filled circles are ASCA values, and diamonds are ROSAT values (Ortolani et al. 1997). Colored lines represent the relative contribution function (the emissivity function multiplied by the EMD at each point). Lower figure: Observed to predicted line ratios for the ion stages in top figure with S/N greater than 3. The broken line denotes a factor of 2.

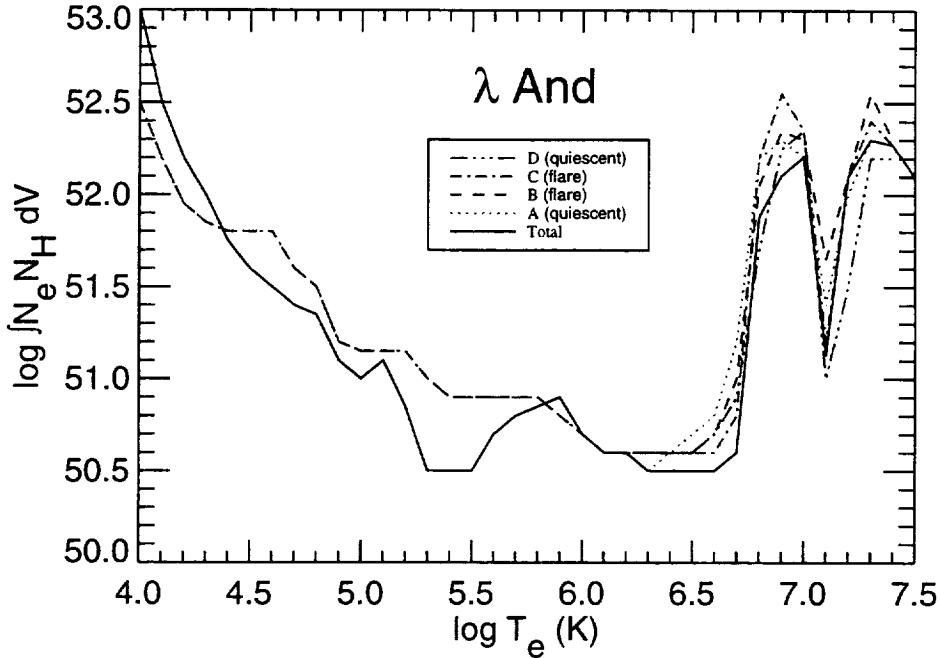


Figure 5. Comparison between the EMD plots for the different segments.

We have estimated the scale size for the feature in which this electron density is measured by substituting the value of the emission measure for Fe XXI $\lambda 102.22$ and $\lambda 128.73$. Assuming a stellar radius of $R_* = 7.5 R_\odot$ (Donati et al. 1995), the emitting volume is $\Delta V = 2.13 \times 10^{27} \text{ cm}^3$, and the scale size factor is $(\Delta V)^{1/3}/R_* = 0.002$

4.3. Emission Measure Distribution

The EMD shows a clear bump around $\log T_e (\text{K}) = 6.9$ and a very small one in $\log T_e (\text{K}) = 5.1$, and seems not to change substantially between the segments. The changes observed on the lines are well explained by this small changes in the EMD between different segments. The EMD is less well defined in the range between $\log T_e (\text{K}) = 5.4$ – 6.5 , where the lack of strong lines results in a more insecure fitting. The dip at $\log T_e (\text{K}) = 7.1$ can be “raised”, but it results in higher error levels, and in any case can not be raised to the same level as the surrounding points. So it confirms the consistency of this bump, also observed in other stars, as 44i Boo or Capella (Brickhouse & Dupree 1998, Dupree et al. 1993), and seems to be very stable when the EMD is fitted for this system even during the flares. The changes observed could be well explained by the presence of more material to form the lines during the flares than in the quiescent segments (as the interval D).

Values obtained by Ortolani et al. (1997) from ASCA and ROSAT data using 2-T models, have been included for comparison with the EUVE data, and

are not noticeably discrepant. Since the 2-T models force all the material to 2 temperatures, the values of the EMD must necessarily be higher than in the continuous models.

5. Conclusions

- Two flares were observed in detail in the light curve, giving the opportunity to analyze separately the spectra coming from quiescent and flare intervals. This analysis showed that the EMD at a given T can vary by a factor of 1.6 to 2.5 among the different segments.
- Fe XXI lines ratios indicate high levels of electron density ($\simeq 5 \times 10^{12} \text{ cm}^{-3}$), evolving to higher values for the flare segments. (The scale of material at $\log T_e \text{ (K)} \sim 7.0$ is much less than a stellar radius).
- The existence of a bump around $\log T_e \text{ (K)} = 6.9$ is necessary, otherwise the predicted fluxes show high error. This bump remains very constant in temperature in the EMD plot at different activity levels, although the value of the EMD varies by a factor of 2.5.
- λ And shows similar features to other active stars (Dupree et al. 1993, Brickhouse & Dupree 1998) with the presence of hot material, an EMD increasing towards coronal temperatures, and a concentration of material around $\log T_e \text{ (K)} \simeq 6.8\text{--}7.0$. A hot tail at $\log T_e \text{ (K)} \simeq 7.2\text{--}7.4$ is also required to produce the observed flux of Fe XXIV.

References

- Baliunas, S.L., Dupree, A.K. 1982, *ApJ*, 252, 66
 Baliunas, S.L., Guinan, E.F., Dupree, A.K. 1984, *ApJ*, 282, 733
 Brickhouse, N.S., Raymond, J.C., Smith, B.W. 1995, *ApJS*, 97, 55
 Brickhouse, N.S., Dupree, A.K. 1998, *ApJ*, 502, 918
 Dempsey, R., Linsky, J.L., Fleming, T.A., Schmitt, J.H.M.M. 1993, *ApJS*, 86, 599
 Donati, J.-F., Henry, G.W., Gall, D.S. 1995, *A&A*, 293, 107
 Dupree, A.K., Brickhouse, N.S., Doschek, G.A., Green, J.C., Raymond, J.C. 1993, *ApJ*, 418, L41
 Henry, G.W., Eaton J.A., Hamer, J. 1995, *ApJS*, 97, 513
 Kimble, R.A., et al. 1993, *ApJ*, 404, 663
 Mitrou, C.K., Mathioudakis, M., Doyle, J.G., Antonopoulou, E., 1997, *A&A*, 317, 776
 Ortolani, A., Maggio, A., Pallavicini, R., Sciortino, S., Drake, J.J., Drake, S.A. 1997, *A&A*, 325, 664
 Osten, R., Brown, A. 1999, *ApJ*, 515, 746
 Perryman, M.A.C., et al. 1997, *A&A*, 323, 49
 Raymond, J.C. 1988, in *Hot Thin Plasmas in Astrophysics*, ed. R. Pallavicini (Dordrecht:Kluwer), 3
 Walker E.C. 1944, *J.R. Astron. Soc. Can.*, 38, 249
 Wood, B.E., Alexander, W.R., Linsky, J.L. 1996, *ApJ*, 470, 1157

1. The first part of the document discusses the importance of maintaining accurate records of all transactions.

2. It also highlights the need for regular audits to ensure the integrity of the data.

3.

4. The second section focuses on the challenges faced by organizations in implementing effective risk management strategies.

5. It explores various factors that can influence the success of these strategies, such as organizational culture and resources.

6.

7. The third part of the document provides a detailed analysis of the current state of the market and its future prospects.

8. It includes a comprehensive overview of the key trends and drivers shaping the industry.

9.

10. The fourth section discusses the role of technology in transforming business operations and improving efficiency.

11. It examines the impact of digitalization on various aspects of the organization, from marketing to customer service.

12.

13. The fifth part of the document addresses the importance of human resources in driving organizational success.

14. It emphasizes the need for a skilled and motivated workforce to achieve long-term growth and innovation.

15.

16. The sixth section explores the role of leadership in shaping the organization's vision and strategy.

17. It discusses the qualities and skills that effective leaders possess and how they can be developed.

18.

19. The seventh part of the document provides a summary of the key findings and recommendations from the study.

20. It offers practical advice for organizations looking to improve their performance and achieve their goals.

21.

22. The eighth section discusses the importance of continuous learning and development for the organization and its employees.

23. It highlights the benefits of investing in training and development programs and how they can lead to improved productivity and innovation.

24.

25. The ninth part of the document provides a detailed analysis of the financial performance of the organization over the past year.

26. It includes a breakdown of the various financial metrics and a comparison with industry benchmarks.

27.

28. The tenth section discusses the role of the board of directors in overseeing the organization's operations and ensuring its long-term success.

29. It examines the responsibilities and duties of the board members and how they can effectively fulfill their roles.

30.

31. The eleventh part of the document provides a summary of the key findings and recommendations from the study.

32. It offers practical advice for organizations looking to improve their performance and achieve their goals.

33.

34. The twelfth section discusses the importance of maintaining accurate records of all transactions.

35. It highlights the need for regular audits to ensure the integrity of the data.

36.

37. The thirteenth part of the document provides a detailed analysis of the current state of the market and its future prospects.

38. It includes a comprehensive overview of the key trends and drivers shaping the industry.

39.

40. The fourteenth section discusses the role of technology in transforming business operations and improving efficiency.

41. It examines the impact of digitalization on various aspects of the organization, from marketing to customer service.

42.

43. The fifteenth part of the document addresses the importance of human resources in driving organizational success.

44. It emphasizes the need for a skilled and motivated workforce to achieve long-term growth and innovation.

45.

46. The sixteenth section explores the role of leadership in shaping the organization's vision and strategy.

47. It discusses the qualities and skills that effective leaders possess and how they can be developed.

48.

49. The seventeenth part of the document provides a summary of the key findings and recommendations from the study.

50. It offers practical advice for organizations looking to improve their performance and achieve their goals.

51.